



Published in final edited form as:

Osteoarthritis Cartilage. 2009 December ; 17(12): 1639–1648. doi:10.1016/j.joca.2009.07.003.

MACROMER DENSITY INFLUENCES MESENCHYMAL STEM CELL CHONDROGENESIS AND MATURATION IN PHOTOCROSSLINKED HYALURONIC ACID HYDROGELS

Isaac E. Erickson^{1,2}, Alice H. Huang^{1,2}, Swarnali Sengupta¹, Sydney Kestle¹, Jason A. Burdick², and Robert L. Mauck^{1,2}

¹McKay Orthopaedic Research Laboratory, Department of Orthopaedic Surgery, University of Pennsylvania, Philadelphia, PA 19104

²Department of Bioengineering, University of Pennsylvania, Philadelphia, PA 19104

Abstract

Objective—Engineering cartilage requires that a clinically relevant cell type be situated within a 3D environment that supports cell viability, the production and retention of cartilage-specific ECM, and eventually, the establishment of mechanical properties that approach that of the native tissue. In this study, we investigated the ability of bone marrow derived mesenchymal stem cells (MSCs) to undergo chondrogenesis in crosslinked methacrylated hyaluronic acid (HA) hydrogels (MeHA) of different macromer concentrations (1, 2, and 5%).

Design—Over a six week culture period under pro-chondrogenic conditions, we evaluated cartilage-specific gene expression, ECM deposition within constructs and released to the culture media, and mechanical properties in both compression and tension. Further, we examined early matrix assembly and long term histological features of the forming tissues, as well as the ability of macromolecules to diffuse within hydrogels as a function of MeHA macromer concentration.

Results—Findings from this study show that variations in macromer density influence MSC chondrogenesis in distinct ways. Increasing HA macromer density promoted chondrogenesis and matrix formation and retention, but yielded functionally inferior constructs due to limited matrix distribution throughout the construct expanse. In 1% MeHA constructs, the equilibrium compressive modulus reached 0.12 MPa and s-GAG content reached nearly 3% of the wet weight, values that matched or exceeded those of control agarose constructs and that are 25% and 50% of native tissue levels, respectively.

Conclusions—These data provide new insight into how early matrix deposition regulates long term construct development, and defines new parameters for optimizing the formation of functional MSC-based engineered articular cartilage using HA hydrogels.

Keywords

Mesenchymal Stem Cells; Photocrosslinked Hydrogels; Chondrogenesis; Mechanical Properties

© 2009 OsteoArthritis Society International. Published by Elsevier Ltd. All rights reserved.

†**Corresponding Author:** Robert L. Mauck, Ph.D., Assistant Professor of Orthopaedic Surgery and Bioengineering, McKay Orthopaedic Research Laboratory, Department of Orthopaedic Surgery, University of Pennsylvania, 36th Street and Hamilton Walk, Philadelphia, PA 19104, Phone: (215) 898-3294, Fax: (215) 573-2133, Email: lemauck@mail.med.upenn.edu.

Publisher's Disclaimer: This is a PDF file of an unedited manuscript that has been accepted for publication. As a service to our customers we are providing this early version of the manuscript. The manuscript will undergo copyediting, typesetting, and review of the resulting proof before it is published in its final citable form. Please note that during the production process errors may be discovered which could affect the content, and all legal disclaimers that apply to the journal pertain.

Introduction

Articular cartilage lines the surfaces of joints and functions to transmit stresses. This function is enabled by the complex interplay between the fluid within the tissue with the dense extracellular matrix (ECM); specifically the type II collagen network and the negatively charged large proteoglycans. Subsequent to trauma, or as a result of degenerative diseases, cartilage undergoes fluctuations in its mechanical and biochemical content, and thus, loses its load-bearing capacity. To address this, the last two decades have witnessed a surge in activity aimed at the formation of engineered cartilage. Much of this work employed articular chondrocytes in three-dimensional (3D) culture environments (see [1] for review). In 3D hydrogels in particular, chondrocytes produce cartilage ECM that is assembled into a functional network with properties that begin to approximate that of native tissue [2]. Physical properties of the gel, including polymer density and crosslinking, control the localization and mechanical properties of newly formed matrix [3,4], as well as the diffusion of large macromolecules [5]. The potential of hydrogels is underscored by recent work showing that compressive properties can meet or exceed native tissue properties (0.5–1.0 MPa) when custom media regimens are employed [6,7].

Despite these promising findings, the clinical use of chondrocytes may have limitations. Aged chondrocytes form mechanically inferior constructs when compared to those derived from juvenile chondrocytes [8,9]. An alternative might be the use of mesenchymal stem cells (MSCs) [10–12], which are expandable and retain their multi-differentiation characteristics [13]. As with chondrocytes, a range of 3D environments have been employed for engineering cartilage with MSCs (e.g., [14–19]). We recently demonstrated that bovine MSCs undergo chondrogenesis in agarose (a thermoreversible hydrogel), in self-assembling peptide gels, and in photocrosslinked hyaluronic acid (HA) hydrogels [20]. Mechanical properties and biochemical content of these constructs increased with time in each hydrogel, though tissue formation was dependent on the type of hydrogel employed.

The literature on MSC differentiation indicates that specific factors modulate the rate and/or extent of MSC chondrogenesis. The biologic interface can induce different levels of molecular level chondrogenesis and control cell shape; inclusion of RGD moieties in modified alginate gels can limit chondrogenesis above a certain threshold [21], while modification of polyethylene glycol (PEG) hydrogels with a collagen mimetic peptide can enhance chondrogenesis [22]. Direct comparisons between photocrosslinked PEG hydrogels (simple, non-interactive) and HA hydrogels (biologic, interactions through CD44 receptors) show improved chondrogenesis in HA when all other factors are held constant [23]. Additionally, biophysical properties such as pore size modulate the extent to which MSCs differentiate and accumulate matrix in PEG-based semi-interpenetrating networks [24]. While not yet shown for chondrogenesis in 3D culture, the micromechanics of the supporting environment can also tune MSC lineage-specification in 2D culture systems [25].

Collectively, these findings suggest that the biological, mechanical, and biophysical properties of the microenvironment interact to control the lineage specification of MSCs, as well as tissue maturation. Our past work with crosslinked HA hydrogels suggests that macromer density (which is inversely related to pore size and directly proportional to bulk mechanical properties) can be used to tune matrix formation by auricular chondrocytes [26]. As our previous findings show that MSCs undergo chondrogenesis in HA gels, but do so to a lesser extent than in other hydrogel environments (such as agarose), the purpose of this study was to determine whether changes in HA macromer density influence ECM deposition and generation of functional cartilage-like properties by MSCs. Results indicated that increasing HA density promoted chondrogenesis and matrix formation and retention, but yielded functionally inferior constructs

due to limited matrix distribution throughout the construct expanse. These data provide new insight into how early matrix deposition regulates long term construct development, and define new parameters for optimizing functional MSC-based engineered cartilage using HA hydrogels.

Materials and Methods

Mesenchymal Stem Cell (MSC) Isolation and Expansion

Bone marrow was extracted from juvenile bovine tibiae (Research 87, Boylston, MA) and MSCs isolated [14]. MSCs were expanded in a basal medium (BM) composed of DMEM supplemented with 10% Fetal Bovine Serum (FBS, Gibco Invitrogen, Carlsbad, CA) and 1% penicillin-streptomycin-fungizone (PSF) through 2–3 passages. Three replicate studies were performed, with MSCs from 2–3 donor animals pooled for each replicate. Each replicate showed similar trends, and data from one replicate is presented.

Fabrication of Acellular and MSC-Seeded Constructs

Photocrosslinkable hyaluronic acid (HA) macromer was synthesized as previously described [27]. Briefly, 65 kDa HA (Lifecore, Chaska, MN) was methacrylated with methacrylic anhydride (Sigma Chemicals, St. Louis, MO). Degree of methacrylation (assessed by NMR [27]) was ~25%. Methacrylated HA (MeHA) solutions were prepared at 1, 2, and 5% (mass/volume) in PBS with 0.05% w/v of the photoinitiator I2959 (2-methyl-1-[4-(hydroxyethoxy) phenyl]-2-methyl-1-propanone, Ciba-Geigy, Tarrytown, NY). For cell-laden gels, MSCs were suspended in MeHA solutions at 20 million cells/mL. Acellular and MSC-laden MeHA macromer suspensions were then cast between glass plates separated by a 2.25 mm spacer and photopolymerized with UV exposure [20]. For controls, agarose hydrogels (Ag, 2.25 mm thick) were formed at 20 million cells/mL [28]. Cylindrical constructs were cored from hydrogel slabs at 4 mm (for MSC-laden gels) or 8 mm (for acellular gels).

Mechanical Characterization of Acellular Constructs

Acellular MeHA disks (Ø5 mm by 2.25 mm) were formed as above and tested in confined compression in a PBS bath [29]. Three sequential ramps of 10% strain (0.05%/second) were applied, and samples were allowed to reach equilibrium between ramps (~1200 seconds). Data from the second ramp (10–20% deformation) were extracted and fit to the Biphasic Theory of Mow and co-workers [30] to determine construct permeability (k) and aggregate modulus (H_A).

Macromolecular Diffusion in Acellular Constructs

Fluorescein-conjugated dextran (70 kDa and 2,000 kDa; Molecular Probes, Invitrogen) was suspended within MeHA (1, 2, and 5%) hydrogels at 175 $\mu\text{g/mL}$ or 85 $\mu\text{g/mL}$, respectively. Gels were maintained in 2 mL of PBS at 37°C on a rocker plate, and supernatant sampled over 72 hours. Released dextran was measured via fluorescence (485 nm/518 nm), with concentration determined from standard curves. The effective ‘diffusivity’ was determined by plotting concentration (normalized to final) versus the square root of time [31].

Long-term Culture Conditions for MSC-Seeded Constructs

Constructs were cultured for up to six weeks (1 mL/construct) in TGF- β 3 (10 ng/mL; R&D Systems, Minneapolis, MN) supplemented, chemically defined medium (CM+). CM consisted of high-glucose DMEM with 1 \times PSF, 0.1 μM dexamethasone, 50 $\mu\text{g/mL}$ ascorbate 2-phosphate, 40 $\mu\text{g/mL}$ L-proline, 100 $\mu\text{g/mL}$ sodium pyruvate, and ITS+ (6.25 mg/mL insulin, 6.25 mg/mL transferrin, 6.25 ng/mL selenous acid, 1.25 mg/mL bovine serum albumin, and 5.35 mg/mL linoleic acid). Media were changed twice weekly.

Viability and Short-term Expression Analysis of MSC-seeded Constructs

For viability assays, samples were tested at 3 and 6 weeks using the LIVE/DEAD staining kit (Molecular Probes, Invitrogen) [20]. Additionally, on days 0, 3, and 21, metabolic activity was quantified with the MTT assay [20]. Briefly, samples were incubated in MTT reagent for 1 hour at 37°C, washed in PBS, and developed color eluted with dimethyl sulfoxide (DMSO), and absorbance read at 540 nm. For gene expression, RNA was extracted from day 0, 1, 7 and 21 samples with two sequential extractions in TRIZOL-chloroform. After quantification of RNA yield and purity, (Nanodrop, Thermo Scientific, Waltham, MA), reverse transcription was carried out with the Superscript First Strand Synthesis System kit (Invitrogen). cDNA amplification was carried out using SYBR Green Master Mix on a 7300 Applied Biosystems real time PCR machine with intron spanning primers. Expression of type I collagen (Col I), type II collagen (Col II) and aggrecan (AGG) were determined and normalized to GAPDH.

Biomechanical Analysis of MSC-seeded Constructs

Compressive equilibrium (E_Y) and dynamic ($|G^*|$) moduli of constructs were determined by unconfined compression between impermeable platens in a PBS bath [29]. Compressive modulus was determined via stress-relaxation testing, and subsequently a 1.0 Hz sinusoidal deformation of 1% was applied and dynamic modulus determined [32]. In a separate study, tensile properties were measured. MSC-seeded samples were fabricated as above, but cut from slabs into strips (4 mm × 20 mm × 1.5 mm), and cultured in CM+ (6 mL per strip). Given the larger size of these samples and the poor findings with 5% HA in compression studies, only 1 and 2% MeHA concentrations were investigated. Samples were tested via a quasi-static extension to failure [28], with the ramp tensile modulus computed from the linear region of the stress-strain curve.

Biochemical Analysis of MSC-seeded Constructs

After testing, construct wet weights were recorded, and DNA, sulfated glycosaminoglycan (s-GAG), and collagen contents assessed [20]. DNA and s-GAG content was determined via Picogreen (Molecular Probes, Eugene, OR) and 1,9-dimethylmethylene blue (DMMB) assays, respectively [33]. Orthohydroxyproline (OHP) content of hydrolyzed digest was measured via reaction with chloramine T and diaminobenzaldehyde [34]. Collagen was extrapolated from OHP using a 1:7.14 ratio of OHP:collagen [35]. In one replicate, s-GAG content of culture medium was measured at each feeding.

Histological Analysis of MSC-seeded Constructs

Constructs were fixed in 4% paraformaldehyde, embedded in paraffin and sectioned (8 μ m). Analysis was carried out on days 3, 5, 7, 10, and 14 and bi-weekly through week 6. Samples were stained for proteoglycans with Alcian blue (pH 1.0) and for collagen via Picrosirius Red [28]. Immunohistochemistry was used to visualize localization of collagen types I and II [28]. Samples underwent antigen retrieval and were sequentially treated at room temperature with 300 mg/mL hyaluronidase (Type IV, Sigma, St. Louis, MO), 3% H₂O₂, and blocking reagent (DAB150 IHC Select, Millipore, Billerica, MA). Sections were then treated with antibodies (5 mg/mL) to type I collagen (MAB3391, Millipore) or type II collagen (11e-116B3, Developmental Studies Hybridoma Bank, Iowa City, IA) in 3% BSA (control sections treated with 3% BSA only). Finally, biotinylated goat anti-rabbit IgG secondary antibody conjugated with streptavidin horseradish peroxidase was localized to primary antibodies, and color developed with DAB chromagen reagent (DAB150 IHC Select, Millipore). Images were acquired at magnifications of 5 or 10X.

Statistical Analysis

Data are reported as the mean and standard deviation; sample numbers are indicated in the associated figure legends. Statistical analysis (SYSTAT 12, Systat Software, Chicago, IL) included both one-way and two-way ANOVA, with gel group (1%, 2%, 5%, Ag) and time in culture as independent variables. When significance ($p < 0.05$) was indicated by ANOVA, Tukey's *post hoc* tests were applied to enable comparisons between groups.

Results

Macromer Density Influences Acellular Hydrogel Mechanics

Prior to cell-seeding studies, crosslinked MeHA hydrogels were formed at varying concentrations (1, 2, and 5%) and tested in confined compression. Increasing macromer concentration led to decreases in construct permeability (k), with both 2% and 5% MeHA hydrogels significantly less permeable than 1% MeHA hydrogels ($p < 0.05$, Figure 1). H_A showed the reverse trend, with 5% MeHA gels significantly stiffer than both 1% and 2% gels ($p < 0.05$).

MSC Viability and Differentiation in HA Gels with Increasing Macromer Density

After ascertaining concentration-dependent differences in hydrogel properties, MSC viability and differentiation was assessed in MeHA gels of increasing macromer concentration (1, 2, and 5%). Viable cells were observed uniformly in all MeHA and Ag constructs on both day 21 and day 42 (Figure 2). There appeared to be more cell clustering with higher MeHA concentrations at both time points. Little evidence of cell death was observed under any condition (data not shown). Metabolic activity showed that, relative to day 1, 1% MeHA and Ag gels increased with time ($p < 0.05$), but after 21 days no significant differences were observed between groups ($p > 0.05$). DNA content per construct was ~20% and ~40% higher after 42 days in 2 and 5% MeHA hydrogels compared to 1% MeHA and Ag hydrogels, respectively ($p < 0.05$).

Expression analysis was performed on MSC-seeded constructs maintained in a chemically defined media supplemented with TGF- β 3. Results indicated that collagen type I expression remained low throughout the 21 day period, at most increasing by a factor of two over this time course. Conversely, collagen type II expression increased dramatically in each condition, and appeared to be a function of macromer density (with levels in 5% MeHA nearly 4-fold greater than in 1% MeHA or Ag) (Figure 3). Aggrecan increased relative to starting levels in each construct by day 7, with generally higher levels of expression observed in the MeHA constructs compared to Ag constructs. For aggrecan, no clear differences were observed between MeHA gels of different concentrations. These data indicate that MSCs are viable in MeHA hydrogels over long periods, that constructs have stable or slightly increased cell content, and that MSCs undergo chondrogenesis in each of these 3D environments.

Construct Dimensional Stability and Biochemical Content

Biochemical content in engineered cartilage is a function of matrix deposition and retention, as well as volumetric space. In low concentration MeHA gels, initial dimensions (diameter and thickness) decreased markedly (Figure 4). This contraction occurred in both acellular and MSC-seeded gels, suggesting that the initial contraction is a function of the gel itself, rather than cell-mediated mechanisms. Acellular and MSC-seeded 1% MeHA constructs contracted by ~10% in thickness and ~20% in diameter over the first day. Conversely, 5% gels increased in thickness by ~5%, with no change in diameter. 2% MeHA constructs were intermediate to these extremes, while Ag constructs did not change, consistent with previous findings. With culture, construct dimensions changed as well; 1% MeHA constructs recovered towards their

original geometry, while 2% and 5% MeHA constructs increased in thickness by ~30%, and in diameter by 10–20%, by day 42. Over this same time course, Ag constructs showed small increases in diameter and thickness.

Biochemical content of constructs was assessed through six weeks of culture. On a per wet weight (ww) basis, 1% MeHA constructs accumulated the highest s-GAG content in MeHA, reaching levels comparable to Ag constructs ($p>0.05$), while 2 and 5% MeHA constructs contained less s-GAG ($p<0.05$, Figure 5A). On Day 42, 1% MeHA and Ag constructs contained ~3% s-GAG per wet weight, while 2% and 5% MeHA constructs contained ~2% s-GAG. Conversely, in terms of total s-GAG per construct, values in 1% MeHA constructs were less than both 2% and 5% MeHA constructs ($p<0.05$; Table 1). s-GAG lost to the culture media was highest for Ag, reaching peak release rates by day 11. 5% MeHA constructs released the least amount s-GAG per day over the first 21 days, with similar release rates from each MeHA construct observed thereafter (Figure 5C). Collagen content showed a similar trend as s-GAG, with the exception of Ag constructs, which contained higher collagen levels (1.4% ww, $p<0.05$) than each of the MeHA constructs by day 42 (1%: 0.7% ww, 2%: 0.3% ww, 5%: 0.4% ww, Figure 5B). In terms of total collagen per construct, Ag constructs contained the highest levels, while the MeHA formulations were not different from one another (Table 1).

Mechanical Properties of MSC-laden Constructs

Differences in biochemical content (and concentration) of ECM resulted in widely different compressive and tensile properties. While all constructs increased in equilibrium and dynamic modulus with time ($p<0.05$), by day 42 the equilibrium modulus of 1% MeHA constructs was ~20% greater than Ag constructs ($p<0.05$, Figure 6A) and more than 100% greater than both 2% and 5% MeHA constructs ($p<0.05$). The dynamic compressive modulus data followed a similar trend, where 1% MeHA constructs were ~20% greater than Ag, and ~5-fold greater than 2% and 5% MeHA constructs ($p<0.05$, Figure 6B). On day 42, the tensile modulus of Ag constructs was ~2-fold higher than that of 1% MeHA ($p<0.05$, Figure 6D), while 1% MeHA constructs were more than 7-fold greater than 2% MeHA constructs ($p<0.05$). Failure strain did not change markedly with culture (Figure 6C).

ECM Deposition and Distribution in MSC-laden Constructs

Histological analysis at early time points showed marked differences in matrix distribution as a function of macromer density (Figure 7). In 5% MeHA constructs, PGs were sequestered into dense rings around cells by day 7. In contrast, 1% MeHA and Ag gels showed a more homogenous distribution of PGs. Similarly, by day 42, PG and collagen was evenly distributed in 1% MeHA and Ag, while intense pericellular localization was evident in 5% MeHA constructs (Figure 8). Collagen type II (Figure 8) showed increased sequestration of this ECM component in the pericellular space in higher macromer concentration MeHA constructs. Consistent with biochemical findings, histological results also show more intense collagen (bulk and type II) staining in Ag constructs compared to all MeHA constructs.

Macromolecular Diffusion in Acellular MeHA Hydrogels

To better understand the mechanism of matrix distribution, we evaluated macromolecular diffusivity of small (70 kDa, on the order of growth factors) and large (2000 kDa, on the order of ECM aggregates) molecules in MeHA gels of varying macromer density. Release rates of 70 kDa dextran from MeHA hydrogels decreased as macromer density increased (Figure 9A). A similar finding was observed with 2000 kDa dextran (Figure 9B). Linear regression to the relative concentration plotted against the square root of time provides a quantitative ‘effective diffusivity’ for comparing these responses. Linear fits captured the data well ($R^2>0.75$) for each macromer density and both dextran sizes. Macromer concentration had a significant effect

on 'effective diffusivity' for both 70 and 2000 kDa dextran. For each increase in macromer concentration, a significant decrease in diffusivity was observed ($p < 0.05$; Figure 9C).

Discussion

Realization of a functional engineered cartilage construct requires that a clinically relevant cell type be situated within a 3D environment that supports cell viability as well as the production and retention of cartilage specific ECM molecules. Further, the encapsulating material must allow assembly of these molecules into a dense network with physiologic mechanical properties. In this work, we investigated the ability of MSCs to undergo chondrogenesis in crosslinked methacrylated HA hydrogels. This hydrogel formulation has several promising attributes; it is a well defined biologic that can be photo-polymerized in situ to fill any sized defect [36]. Our previous studies with this gel at one macromer concentration (2%) established that MSCs undergo chondrogenesis in MeHA, but also indicated that the rate and extent of functional maturation was reduced when compared to agarose [20]. As MeHA macromer density influences ECM deposition by auricular chondrocyte seeded HA gels [26], this study specifically investigated how variations in this parameter influence the maturation of MSC-based constructs. Results from this study demonstrate that two competing effects occur as macromer density increases: enhanced chondrogenesis that is countermanded by biophysical impediments to distributed matrix assembly.

As previously noted for MeHA [26], and consistent with other hydrogels [37], changes in macromer density had marked effects on the mechanical properties; constructs with higher macromer densities were stiffer. Despite the increasing gel density, viability and DNA assays indicated that cells survive and divide throughout the material. Encapsulated MSCs increased expression of cartilage-specific matrix and accumulated increasing amounts of proteoglycan through 42 days. Despite the hindered diffusion observed for 70 kDa molecules, histological analysis (staining for PG deposition) showed that chondrogenesis occurred throughout the gel, and was not restricted to the periphery in higher macromer concentrations. These findings suggest that the HA gels support viability and MSC chondrogenesis at all macromer concentrations.

The enhanced chondrogenic differentiation and PG observed in higher macromer concentration MeHA constructs could arise from a number of different factors. First, we have previously shown that MeHA hydrogels enhance molecular level chondrogenesis compared to inert crosslinked networks such as PEG [23]. HA is a component of the native cartilage ECM and so the gel presents a biologic interface with which both chondrocytes and MSCs can interact (through CD44 receptors) [38]. In high macromer constructs, a greater probability of receptor mediated interaction with the material exists, just as concentration dependent effects are observed when RGD is coupled to otherwise biologically inert hydrogels [21]. Alternatively, the higher stiffness of the material may influence differentiation. Findings in monolayer studies suggest that MSCs can interpret the microenvironmental stiffness to modulate differentiation [39]. Here, increasing macromer density increases gel stiffness; MSCs may respond to this by increasing the degree to which they undergo chondrogenesis. Still another possibility relates to the rapid and intense accumulation of newly formed matrix in the pericellular space in higher density MeHA. While a high local PG concentration exerts negative feedback on further PG production by chondrocytes [2], this does not seem to be the case with MSCs in this system. Rather, the ECM in the pericellular space may act to concentrate locally produced factors (ECM to which the cells bind, or growth factors that themselves bind to ECM), creating a microenvironment that better supports and/or maintains chondrogenesis. Future studies will be required to elucidate the precise mechanism by which this enhanced differentiation occurs in higher density MeHA gels.

Despite the anabolic and/or pro-chondrogenic effects of increasing MeHA macromer density, these positive findings were counterbalanced by the limited diffusion of large ECM molecules away from their origin. This limitation impeded the homogenous distribution of formed ECM, and so hampered the functional maturation. This is consistent with the findings of Buxton and colleagues, who showed that inclusion of spacers within PEG gels allowed for greater matrix distribution by human MSCs [24] and by Ng and colleagues using bovine chondrocytes in an agarose system [37]. While 5% MeHA constructs produced and retained the highest absolute amount of PG, they failed to develop increasing mechanical properties compared to lower macromer concentration constructs that produced lesser amounts of PG. This is partially due to volumetric changes observed; 1% MeHA constructs made less PG, but contracted slightly and so concentrated the formed ECM, while 5% MeHA constructs made and retained more PG, but swelled significantly. These findings suggest that new methods must be developed to take advantage of the positive features of a higher MeHA concentration, while increasing the mobility of newly formed matrix. For example, Bryant and colleagues have shown greater ECM distribution in chondrocyte-seeded PEG gels that contain degradable linkages [40], and Park and co-workers have shown similar findings in MMP-cleavable hydrogels [41]. Working with a new hydrolytically degradable version of these crosslinked HA hydrogels, we have recently shown that crosslink degradation leads to more rapid dispersion of ECM in short term MSC studies [42]. It is not yet clear how long the pro-chondrogenic signal provided by the HA microenvironment (be it stiffness or biologic moieties) must be present to result in long term increases in matrix production. In future studies, it will be critical to carefully tune early matrix assembly, and the positive benefits thereof, with long term requirements for matrix elaboration.

The results of this study are promising, in that they show a clear macromer density dependent development of construct mechanical properties. The equilibrium and dynamic compressive properties of MSC-seeded 1% MeHA constructs match or exceed properties achieved with Ag hydrogels seeded with the same MSC population and maintained identically. Indeed, equilibrium compressive properties and s-GAG content reach 25% and 50% of native tissue levels, respectively. However, collagen content in MeHA gels remains low, and is lower than that produced in Ag constructs. This is a significant finding, as collagen content correlates well with tensile properties in native tissue and engineered constructs. In this study, the tensile properties of 1% MeHA constructs remained significantly lower than Ag constructs. Further, it should be noted that the compressive mechanical properties (even in Ag hydrogels) remain lower than that produced by native chondrocytes in Ag hydrogels [14]. This is consistent with the idea that MSCs remain incompletely (or inefficiently) committed to the chondrocyte phenotype, even in MeHA.

Despite these limitations, these data provide new insight into how early matrix deposition regulates long term construct development, and define new parameters for optimizing the formation of functional MSC-based engineered cartilage using HA hydrogels. For example, in the case of higher density MeHA constructs, dynamic loading might be used to further matrix distribution. Theoretical and experimental results suggest that dynamic loading can expedite the movement of large molecules in dense hydrogels [5,43]. Such an approach may be useful in coupling the pro-chondrogenic/matrix formation events in MeHA hydrogels, while still providing a mechanism for distribution of newly formed constituents throughout the construct, potentially improving bulk mechanical properties. Taken together, these results provide new evidence that HA hydrogels support the functional chondrogenesis of MSCs, with mechanical properties matching or exceeding our best results to date in other hydrogel systems. With further optimization, this material holds tremendous promise in the fabrication of functional cartilage replacements to restore function to damaged or diseased native tissue.

Acknowledgments

This work was supported by the National Institutes of Health (RO3 AR053668, K22 DE015761, and RO1 EB008722), the Penn Center for Musculoskeletal Disorders (AR050950), the Penn Institute on Aging, and the National Science Foundation. Additional support was from an NSF-sponsored REU program through the Nano-Bio Interface Center (NBIC) at the University of Pennsylvania. The authors would like to thank Ms. Cindy Chung for assistance with MeHA synthesis and Mr. Andy Liang for assistance with tensile testing. The type II collagen antibody developed by Thomas F. Linsenmayer was obtained from the Developmental Studies Hybridoma Bank developed under the auspices of the NICHD and maintained by the University of Iowa, Department of Biology, Iowa City, IA 52242.

References

1. Chung C, Burdick JA. Engineering cartilage tissue. *Adv Drug Deliv Rev* 2008;60:243–262. [PubMed: 17976858]
2. Buschmann MD, Gluzband YA, Grodzinsky AJ, Kimura JH, Hunziker EB. Chondrocytes in agarose culture synthesize a mechanically functional extracellular matrix. *J Orthop Res* 1992;10:745–758. [PubMed: 1403287]
3. Bryant SJ, Nuttelman CR, Anseth KS. The effects of crosslinking density on cartilage formation in photocrosslinkable hydrogels. *Biomed Sci Instrum* 1999;35:309–314. [PubMed: 11143369]
4. Ng KW, Mauck RL, Statman LY, Lin EY, Ateshian GA, Hung CT. Dynamic deformational loading results in selective application of mechanical stimulation in a layered, tissue-engineered cartilage construct. *Biorheology* 2006;43:497–507. [PubMed: 16912421]
5. Albro MB, Chahine NO, Li R, Yeager K, Hung CT, Ateshian GA. Dynamic loading of deformable porous media can induce active solute transport. *J Biomech* 2008;41:3152–3157. [PubMed: 18922531]
6. Byers BA, Mauck RL, Chiang IE, Tuan RS. Transient exposure to transforming growth factor beta 3 under serum-free conditions enhances the biomechanical and biochemical maturation of tissue-engineered cartilage. *Tissue Eng Part A* 2008;14:1821–1834. [PubMed: 18611145]
7. Lima EG, Bian L, Ng KW, Mauck RL, Byers BA, Tuan RS, et al. The beneficial effect of delayed compressive loading on tissue-engineered cartilage constructs cultured with TGF-beta3. *Osteoarthritis Cartilage* 2007;15:1025–1033. [PubMed: 17498976]
8. Tallheden T, Bengtsson C, Brantsing C, Sjogren-Jansson E, Carlsson L, Peterson L, et al. Proliferation and differentiation potential of chondrocytes from osteoarthritic patients. *Arthritis Res Ther* 2005;7:R560–R568. [PubMed: 15899043]
9. Tran-Khanh N, Hoemann CD, McKee MD, Henderson JE, Buschmann MD. Aged bovine chondrocytes display a diminished capacity to produce a collagen-rich, mechanically functional cartilage extracellular matrix. *J Orthop Res* 2005;23:1354–1362. [PubMed: 16048738]
10. Prockop DJ. Marrow stromal cells as stem cells for nonhematopoietic tissues. *Science* 1997;276:71–74. [PubMed: 9082988]
11. Pittenger MF, Mackay AM, Beck SC, Jaiswal RK, Douglas R, Mosca JD, et al. Multilineage potential of adult human mesenchymal stem cells. *Science* 1999;284:143–147. [PubMed: 10102814]
12. Johnstone B, Hering TM, Caplan AI, Goldberg VM, Yoo JU. In vitro chondrogenesis of bone marrow-derived mesenchymal progenitor cells. *Exp Cell Res* 1998;238:265–272. [PubMed: 9457080]
13. Baksh D, Song L, Tuan RS. Adult mesenchymal stem cells: characterization, differentiation, and application in cell and gene therapy. *J Cell Mol Med* 2004;8:301–316. [PubMed: 15491506]
14. Mauck RL, Yuan X, Tuan RS. Chondrogenic differentiation and functional maturation of bovine mesenchymal stem cells in long-term agarose culture. *Osteoarthritis Cartilage* 2006;14:179–189. [PubMed: 16257243]
15. Awad HA, Wickham MQ, Leddy HA, Gimble JM, Guilak F. Chondrogenic differentiation of adipose-derived adult stem cells in agarose, alginate, and gelatin scaffolds. *Biomaterials* 2004;25:3211–3222. [PubMed: 14980416]
16. Li WJ, Tuli R, Okafor C, Derfoul A, Danielson KG, Hall DJ, et al. A three-dimensional nanofibrous scaffold for cartilage tissue engineering using human mesenchymal stem cells. *Biomaterials* 2005;26:599–609. [PubMed: 15282138]

17. Erickson GR, Gimble JM, Franklin DM, Rice HE, Awad H, Guilak F. Chondrogenic potential of adipose tissue-derived stromal cells in vitro and in vivo. *Biochem Biophys Res Commun* 2002;290:763–769. [PubMed: 11785965]
18. Meinel L, Hofmann S, Karageorgiou V, Zichner L, Langer R, Kaplan D, et al. Engineering cartilage-like tissue using human mesenchymal stem cells and silk protein scaffolds. *Biotechnol Bioeng* 2004;88:379–391. [PubMed: 15486944]
19. Betre H, Ong SR, Guilak F, Chilkoti A, Fermor B, Setton LA. Chondrocytic differentiation of human adipose-derived adult stem cells in elastin-like polypeptide. *Biomaterials*. 2005
20. Erickson IE, Huang AH, Chung C, Li RT, Burdick JA, Mauck RL. Differential Maturation and Structure-Function Relationships in MSC- and Chondrocyte-Seeded Hydrogels. *Tissue Eng Part A*. 2009
21. Connelly JT, Garcia AJ, Levenston ME. Inhibition of in vitro chondrogenesis in RGD-modified three-dimensional alginate gels. *Biomaterials* 2007;28:1071–1083. [PubMed: 17123602]
22. Lee HJ, Yu C, Chansakul T, Hwang NS, Varghese S, Yu SM, et al. Enhanced chondrogenesis of mesenchymal stem cells in collagen mimetic peptide-mediated microenvironment. *Tissue Eng Part A* 2008;14:1843–1851. [PubMed: 18826339]
23. Chung C, Burdick JA. Influence of three-dimensional hyaluronic Acid microenvironments on mesenchymal stem cell chondrogenesis. *Tissue Eng Part A* 2009;15:243–254. [PubMed: 19193129]
24. Buxton AN, Zhu J, Marchant R, West JL, Yoo JU, Johnstone B. Design and characterization of poly (ethylene glycol) photopolymerizable semi-interpenetrating networks for chondrogenesis of human mesenchymal stem cells. *Tissue Eng* 2007;13:2549–2560. [PubMed: 17655489]
25. Engler AJ, Sen S, Sweeney HL, Discher DE. Matrix elasticity directs stem cell lineage specification. *Cell* 2006;126:677–689. [PubMed: 16923388]
26. Chung C, Mesa J, Randolph MA, Yaremchuk M, Burdick JA. Influence of gel properties on neocartilage formation by auricular chondrocytes photoencapsulated in hyaluronic acid networks. *J Biomed Mater Res A* 2006;77:518–525. [PubMed: 16482551]
27. Burdick JA, Chung C, Jia X, Randolph MA, Langer R. Controlled degradation and mechanical behavior of photopolymerized hyaluronic acid networks. *Biomacromolecules* 2005;6:386–391. [PubMed: 15638543]
28. Huang AH, Yeger-McKeever M, Stein A, Mauck RL. Tensile properties of engineered cartilage formed from chondrocyte- and MSC-laden hydrogels. *Osteoarthritis Cartilage* 2008;16:1074–1082. [PubMed: 18353693]
29. Mauck RL, Soltz MA, Wang CC, Wong DD, Chao PH, Valhmu WB, et al. Functional tissue engineering of articular cartilage through dynamic loading of chondrocyte-seeded agarose gels. *J Biomech Eng* 2000;122:252–260. [PubMed: 10923293]
30. Mow VC, Kuei SC, Lai WM, Armstrong CG. Biphasic creep and stress relaxation of articular cartilage in compression? Theory and experiments. *J Biomech Eng* 1980;102:73–84. [PubMed: 7382457]
31. Quinn TM, Kocian P, Meister JJ. Static compression is associated with decreased diffusivity of dextrans in cartilage explants. *Arch Biochem Biophys* 2000;384:327–334. [PubMed: 11368320]
32. Park S, Nicoll SB, Mauck RL, Ateshian GA. Cartilage Mechanical Response under Dynamic Compression at Physiological Stress Levels Following Collagenase Digestion. *Ann Biomed Eng*. 2008
33. Farndale RW, Buttle DJ, Barrett AJ. Improved quantitation and discrimination of sulphated glycosaminoglycans by use of dimethylmethylene blue. *Biochim Biophys Acta* 1986;883:173–177. [PubMed: 3091074]
34. Stegemann H, Stalder K. Determination of hydroxyproline. *Clin Chim Acta* 1967;18:267–273. [PubMed: 4864804]
35. Neuman RE, Logan MA. The Determination of Hydroxyproline. *Journal of Biological Chemistry* 1950;184:299–306. [PubMed: 15421999]
36. Nettles DL, Vail TP, Morgan MT, Grinstaff MW, Setton LA. Photocrosslinkable hyaluronan as a scaffold for articular cartilage repair. *Ann Biomed Eng* 2004;32:391–397. [PubMed: 15095813]
37. Ng KW, Wang CC, Mauck RL, Kelly TA, Chahine NO, Costa KD, et al. A layered agarose approach to fabricate depth-dependent inhomogeneity in chondrocyte-seeded constructs. *J Orthop Res* 2005;23:134–141. [PubMed: 15607885]

38. Knudson CB, Knudson W. Hyaluronan and CD44: modulators of chondrocyte metabolism. *Clin Orthop Relat Res* 2004;S152–S162. [PubMed: 15480059]
39. Engler AJ, Sweeney HL, Discher DE, Schwarzbauer JE. Extracellular matrix elasticity directs stem cell differentiation. *J Musculoskelet Neuronal Interact* 2007;7:335. [PubMed: 18094500]
40. Bryant SJ, Anseth KS. Controlling the spatial distribution of ECM components in degradable PEG hydrogels for tissue engineering cartilage. *J Biomed Mater Res A* 2003;64:70–79. [PubMed: 12483698]
41. Park Y, Lutolf MP, Hubbell JA, Hunziker EB, Wong M. Bovine primary chondrocyte culture in synthetic matrix metalloproteinase-sensitive poly(ethylene glycol)-based hydrogels as a scaffold for cartilage repair. *Tissue Eng* 2004;10:515–522. [PubMed: 15165468]
42. Sahoo S, Chung C, Khetan S, Burdick JA. Hydrolytically degradable hyaluronic acid hydrogels with controlled temporal structures. *Biomacromolecules* 2008;9:1088–1092. [PubMed: 18324776]
43. Mauck RL, Hung CT, Ateshian GA. Modeling of neutral solute transport in a dynamically loaded porous permeable gel: implications for articular cartilage biosynthesis and tissue engineering. *J Biomech Eng* 2003;125:602–614. [PubMed: 14618919]

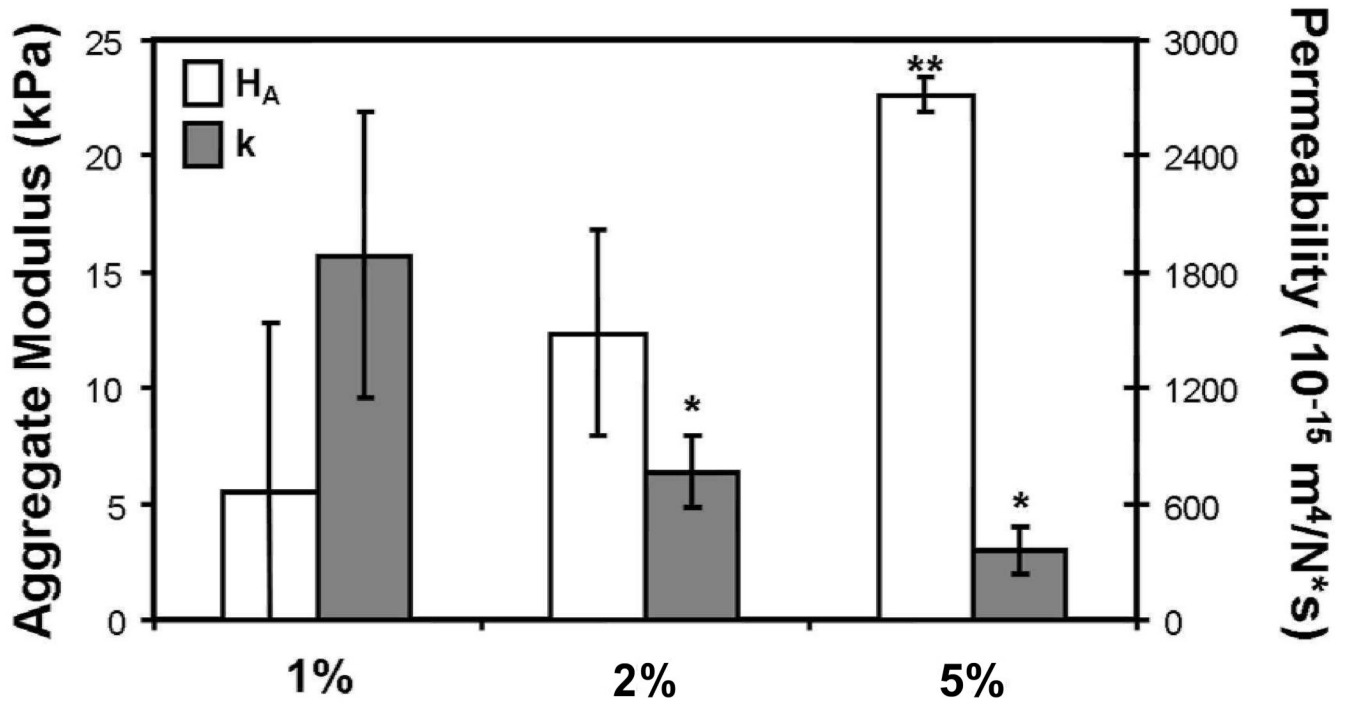


Figure 1. Biphasic parameters of permeability (k) and aggregate modulus (H_A) for MeHA gels with increasing macromer density. ($R^2 > 0.89$; $n = 3-4$ /group; * indicates $p < 0.05$ vs. 1%; ** indicates $p < 0.05$ vs. 1% and 2%)

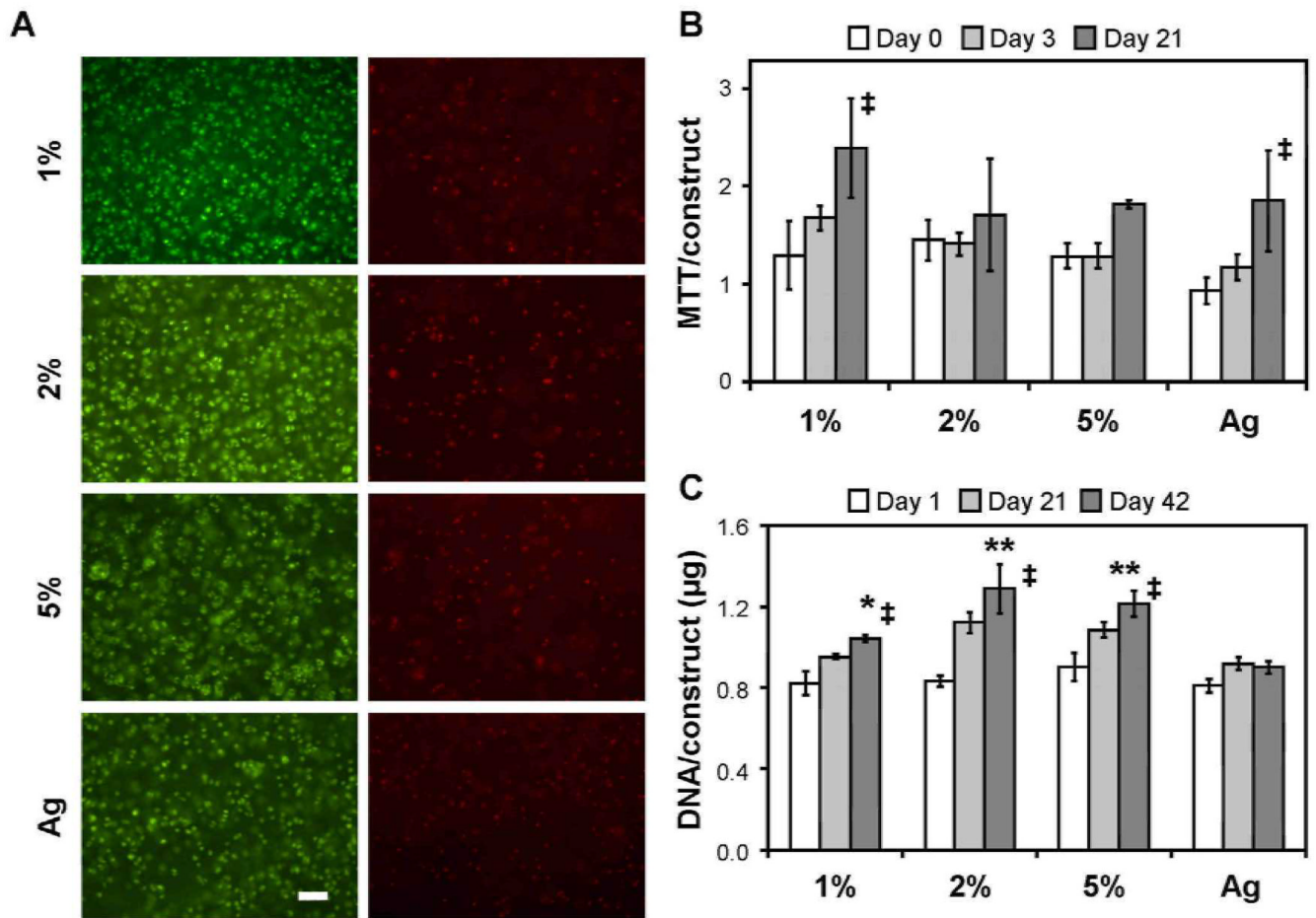


Figure 2.

(A) Live (green, left) and dead (red, right) MSCs in 1%, 2%, and 5% MeHA, and Ag hydrogels 21 days after encapsulation (10X magnification; 200 μ m scale bar). (B) Mitochondrial activity of constructs through day 21. (C) DNA content of MSC-seeded constructs through day 42. (n=4/group/time point, ** indicates p<0.05 vs. 1% and Ag on day 42, * indicates p<0.05 vs. Ag on day 42; ‡ indicates p<0.05 vs. day 0)

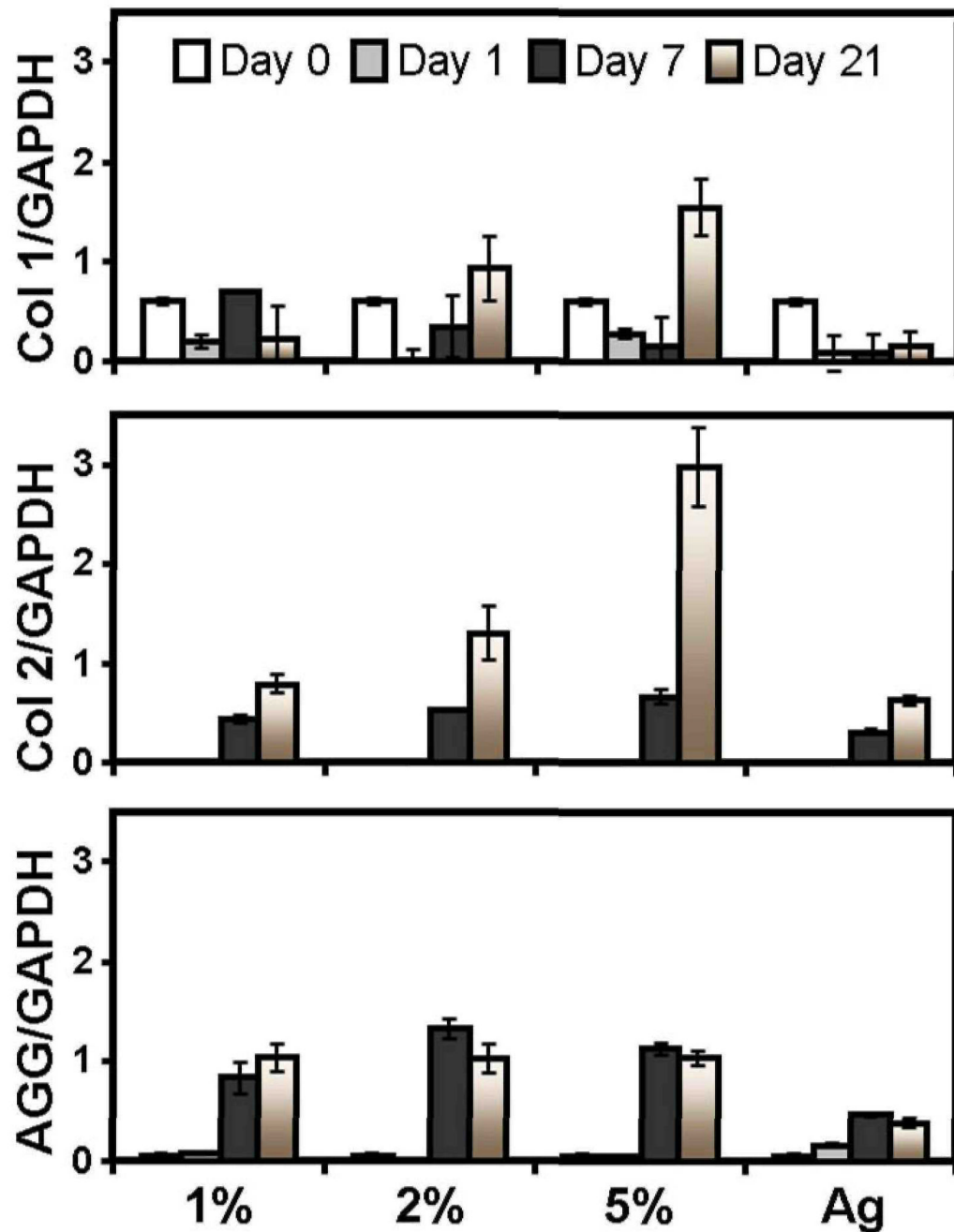


Figure 3.

Collagen type I (top), collagen type II (middle), and aggrecan (bottom) mRNA levels in MSC-seeded MeHA (1%, 2%, and 5%) and Ag constructs through 21 days of chondrogenic culture. Note modest changes in collagen I expression with time and robust increases in collagen II and aggrecan, indicative of chondrogenic differentiation.

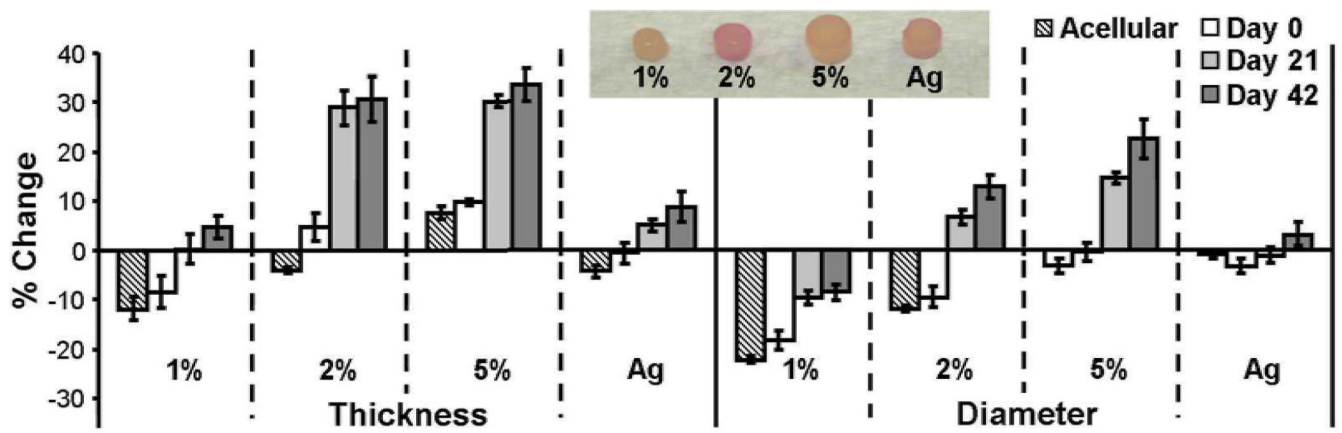


Figure 4. Dimensional variation in acellular and MSC-seeded constructs with time in culture. Differences shown as the percentage of initial size (4 mm diameter and 2.25 mm thickness, n=4/group/time point). Inset image of MSC-seeded constructs after 6 weeks of in vitro culture in chondrogenic medium.

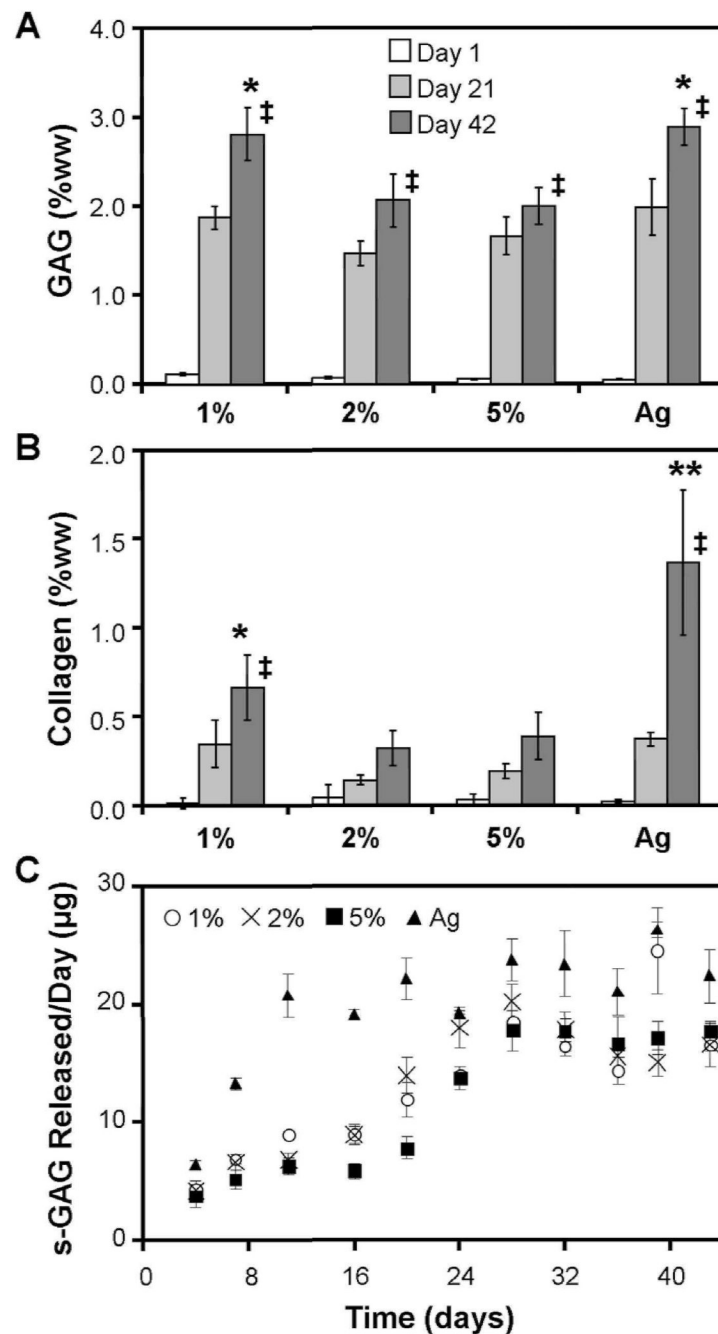


Figure 5.

A) s-GAG percent wet weight (% ww) in 1, 2, and 5% MeHA, and Ag constructs through 42 days of *in vitro* chondrogenic culture. (* indicates $p < 0.05$ vs 2% and 5% MeHA at day 42) B) Collagen content (% ww) in MeHA and Ag constructs through 42 days of culture. (** indicates $p < 0.05$ vs all other groups at day 42, * indicates $p < 0.05$ vs. 2% MeHA) Increased concentration of ECM was observed in Ag and 1% MeHA hydrogels by day 42. ($n=4$ /group/time point, ‡ $p < 0.05$ vs. day 0) C) s-GAG release per day per construct for MSC-seeded MeHA and Ag constructs through 42 days of culture.

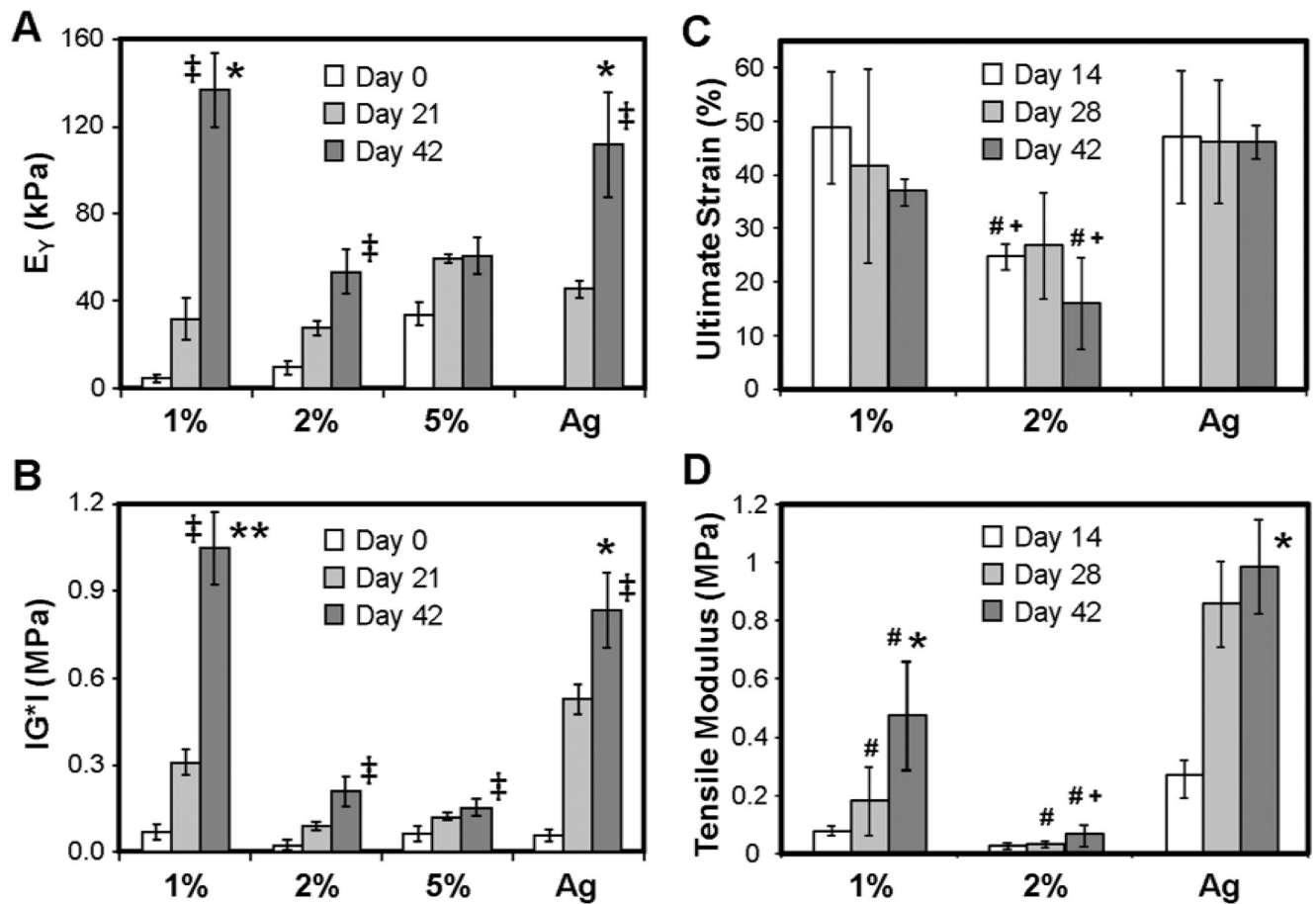


Figure 6.

Equilibrium compressive modulus (A) and dynamic modulus (B) of MeHA and Ag hydrogels through 6 weeks of culture (** indicates $p < 0.05$ vs. all other groups at day 42; * indicates $p < 0.05$ vs. 2% and 5% MeHA). Failure strain (C) and tensile modulus (D) of MSC-seeded 1 and 2% MeHA and Ag constructs at 2, 4, and 6 weeks. (* indicates $p < 0.05$ vs. all other groups on the terminal time point (day 42); # indicates $p < 0.05$ vs. Ag group at same time point; + indicates $p < 0.05$ vs. 1% MeHA group at same time point) Biomechanical properties increase more rapidly and to a higher level in lower concentration MeHA constructs. ($n=4$ /group/time point, ‡ $p < 0.05$ vs. day 0)

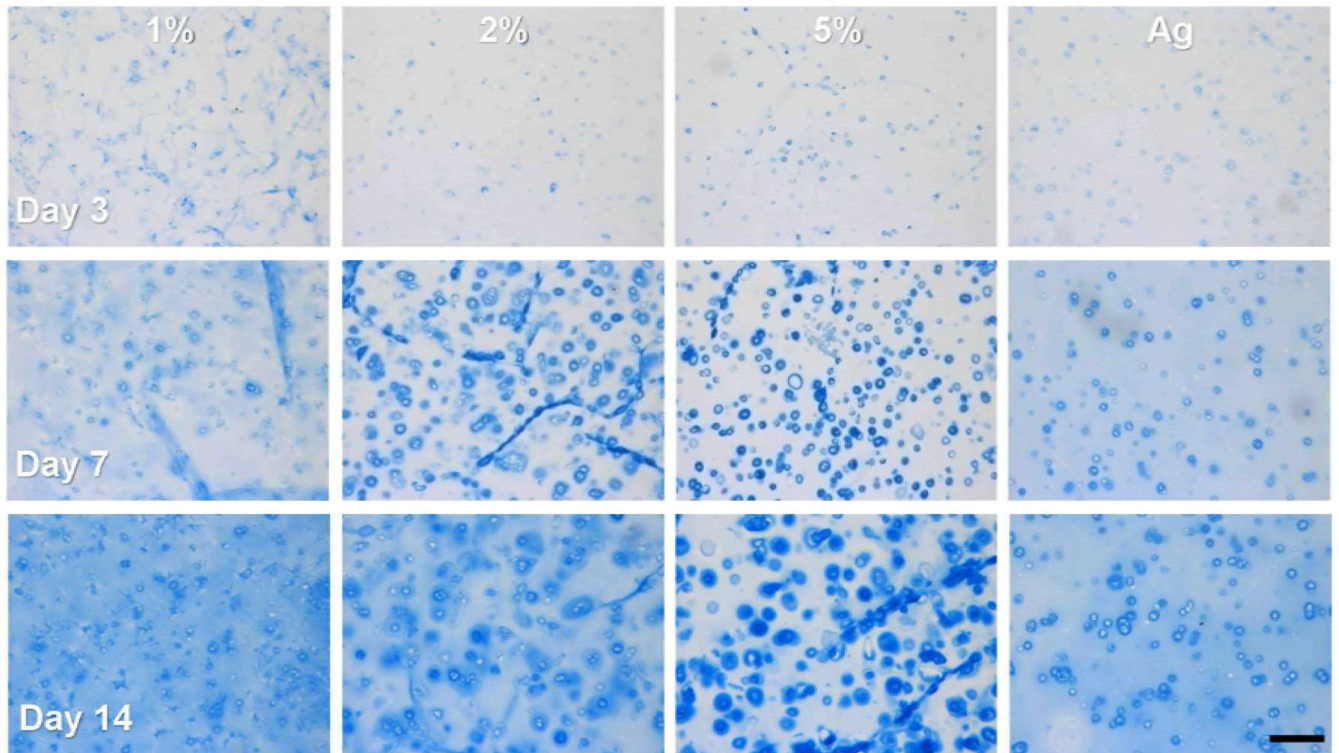


Figure 7. Alcian Blue stained sections of MSC-seeded 1, 2, and 5% MeHA and Ag constructs after 3 (top), 7 (middle), and 14 days (bottom) of chondrogenic culture (10X magnification). Pericellular aggregation of PGs is evident in higher % MeHA constructs in contrast to a more even distribution in 1% MeHA constructs and Ag controls. (Scale bar = 250 μ m)

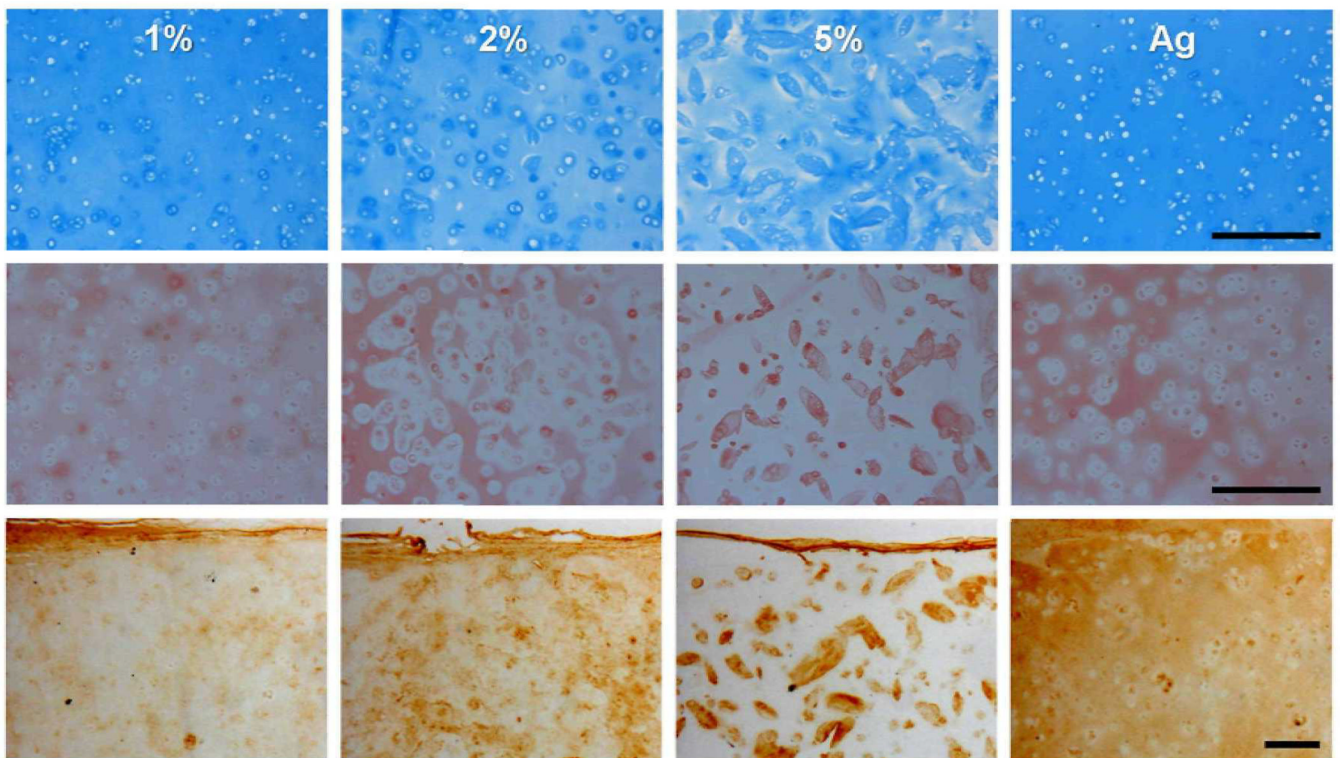


Figure 8. Alcian blue (top) and Picosirius red (middle) stained sections from 1, 2, and 5% MeHA and Ag constructs (10X magnification) on day 42. Collagen type II immunostaining (bottom) on day 42 (5X). Note the dependence of PG and collagen distribution on MeHA macromer concentration. (Scale bar = 250 μ m)

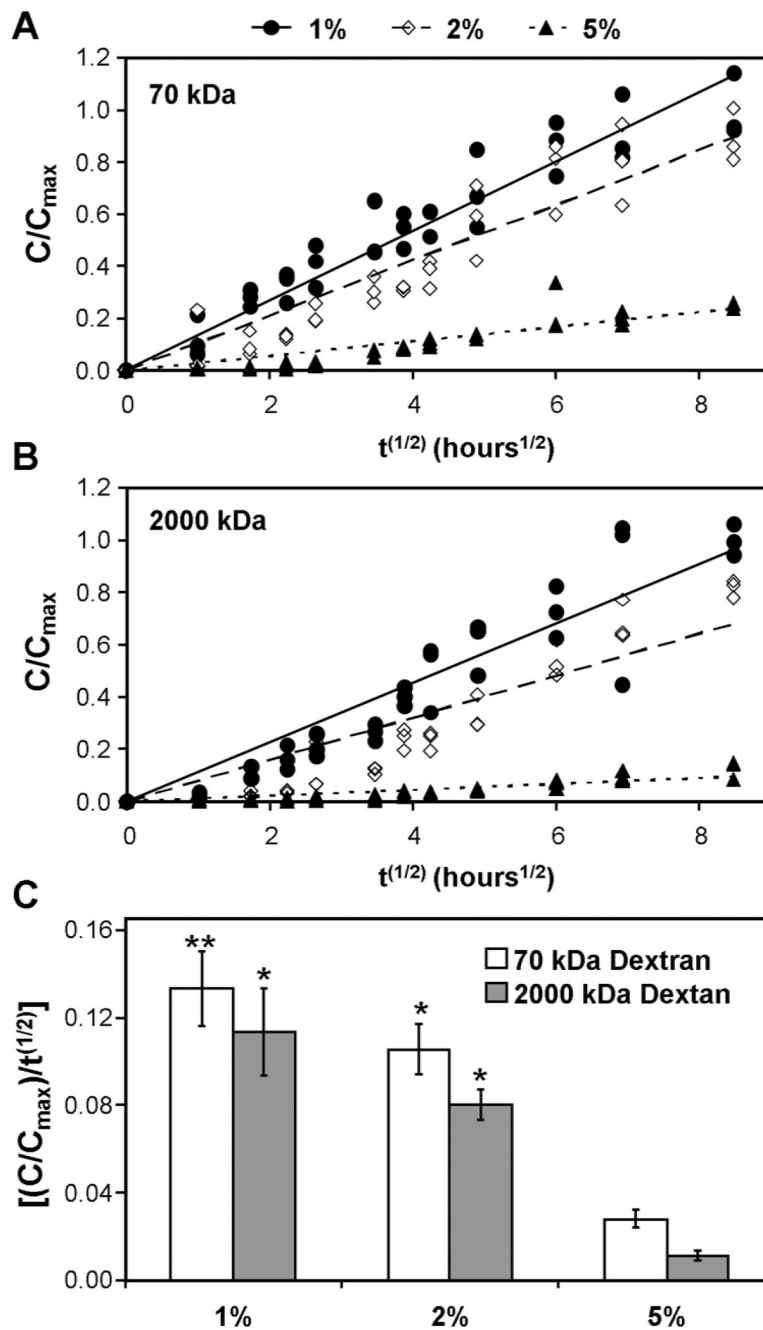


Figure 9. Time course of release of 70 kDa (A) and 2000 kDa (B) fluorescein-conjugated dextran from 1, 2, and 5% MeHA hydrogels (normalized to maximum concentration from 1% MeHA for a given dextran molecular weight). Effective diffusivity (C) of dextran of both sizes decreased with increasing MeHA macromer concentration. (n=3/group; ** indicates p<0.05 vs. both 2% and 5% MeHA groups; * indicates p<0.05 vs. the 5% MeHA group only)

Dimensional, biochemical, and mechanical properties of MSC-seeded MeHA and Ag constructs after 6 weeks of culture (mean \pm standard deviation (SD); n=3–4/group).

Table 1

	1% MeHA		2% MeHA		5% MeHA		2% Agarose	
	mean \pm SD		mean \pm SD		mean \pm SD		mean \pm SD	
Dimensions	Thickness (mm)	2.360.05	2.940.10	3.010.08	2.450.07			
	Diameter (mm)	3.660.06	4.520.10	4.900.16	4.120.10			
Wet Weight (mg)	26.350.72	49.921.83	62.040.75	33.071.05				
Biochemistry	DNA per construct (μ g)	1.040.02	1.290.12	1.220.06	0.900.03			
	Collagen per DNA	167.4045.50	124.7840.56	203.4675.80	499.68142.89			
	Collagen per construct (μ g)	176.1749.49	160.6652.55	240.1880.85	444.79132.61			
	Collagen % _{ww}	0.660.18	0.320.10	0.390.13	1.370.41			
	GAG per DNA	707.7354.25	800.4799.27	1019.4570.36	1058.9273.77			
	GAG per construct (μ g)	739.1462.73	1024.67107.62	1241.54132.43	956.2588.50			
GAG % _{ww}	2.810.30	2.060.30	2.000.20	2.890.21				
Mechanics	E _v (kPa)	136.6617.07	53.579.78	60.808.25	111.9623.96			
	IG ¹ (MPa)	1.050.12	0.210.05	0.160.03	0.830.13			
	Tensile Modulus (kPa)	473.60187.52	63.5036.78	----	991.48162.25			